# A Theoretical Study on the Photochemical Reaction of Carbon Suboxide with Ethylene

**Tsutomu Minato,[1a] Yoshihiro Osamura,[1b] Shinichi Yamabe,[1c] and Kenichi Fukui*[1a]**

*Contribution from the Faculty of Engineering, Kyoto University, Sakyo-ku, Kyoto 606, Japan, the Department of Chemistry, Faculty of Science, Osaka City University, Sumiyoshi-ku, Osaka 558, Japan, and the Department of Chemistry, Nara University of Education, Takabatake-cho, Nara 630, Japan.*
*Received June 18, 1979*

**Abstract:** The photochemical reaction of carbon suboxide with ethylene is studied theoretically in terms of state correlation diagrams and an ab initio calculation. In light of the calculated results, the reaction is suggested to consist of the following processes. Starting from the second excited state of carbon suboxide, the ground-state carbonylcarbene (triplet) is yielded through the bent dissociation path. The carbonylcarbene adds to ethylene in the "bent-in-plane" path, producing cyclopropylideneketene. The cyclopropylideneketene is decomposed through the bent-in-plane path into cyclopropylidene and carbon monoxide. Finally, the cyclopropylidene collapses to form the ground-state allene. The mechanisms of these reactions are elucidated by the mode of orbital interaction.

## I. Introduction

Carbon suboxide ($C_3O_2$) is known to undergo a photochemical reaction with olefin.[2] The single carbon atom of $C_3O_2$ is inserted into the olefinic double bond, yielding an allene ($C_3H_4$) and two molecules of carbon monoxide (CO). The overall reaction of $C_3O_2$ with ethylene ($C_2H_4$) is given as follows:

$$C_3O_2 + C_2H_4 \rightarrow C_3H_4 + 2CO$$

When $C_3O_2$ is labeled in the central position (C*), the newly inserted atom is found in the central position of $C_3H_4$.[3] The reactive intermediate is probably either a carbonylcarbene ($C_2O$) molecule or a free carbon atom. Energy consideration, based on the estimated heat of formation for $C_3O_2$, rules out the possibility of a free carbon atom.[4] The general reaction scheme involving $C_2O$ is represented as follows.

$$O{=}C{=}C^*{=}C{=}O \rightarrow C^*{=}C{=}O + C{=}O \quad (1)$$

$$C^*{=}C{=}O + C_2H_4 \rightarrow CH_2{=}C^*{=}CH_2 + CO \quad (2)$$

Williamson and Bayes pointed out that the photolysis (at 3000 and 2500 Å) shown in eq 1 produced two different intermediates which were thought to be $C_2O(^3\Sigma^-)$ and $C_2O(^1\Delta)$.[5] When they react with olefin as shown in eq 2, $C_2O(^3\Sigma^-)$ displays an electrophilic character but $C_2O(^1\Delta)$ is quite indiscriminate. In the reaction of $C_2O(^3\Sigma^-)$ with olefin, a second intermediate was postulated by Willis and Bayes.[6] While the identification was not certain, they suggested that it was either cyclopropylidene (CP) or cyclopropylideneketene (CK).

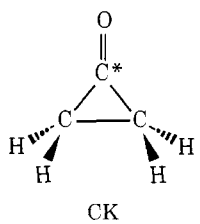

CK

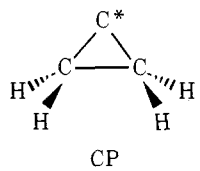

CP

Although it is well accepted that the first step of the photoreaction of $C_3O_2$ with olefin is the dissociation of $C_3O_2$ and the pathway of $C_3O_2(^3\Delta_u) \rightarrow C_2O(^3\Sigma^-) + CO$ has been traced theoretically,[7] the reaction mechanism of the second step represented by eq 2 still involves some doubt. In the present work, the path and the mechanism of the reaction of $C_2O$ with olefin are explored. While the search for the dissociation path of eq 1 is rather straightforward by use of the energy-optimization procedure, the reaction of eq 2 must be analyzed carefully. This is because the reaction may involve several processes such as additions and dissociations and one or more intermediates (e.g., CP and CK). In order to analyze the mechanism of reaction 2, the state correlation diagrams for various processes are drawn systematically and these reaction paths are qualitatively predicted. Based on this prediction, the minimum-energy paths are traced by an ab initio calculation. In this work the reaction starting from the $^3\Sigma^-$ state of $C_2O$ is dealt with, since the calculation for the $^1\Delta$ state of $C_2O$ is technically somewhat difficult.

## II. Consideration of Reaction Paths Based on the State Correlation Diagram

To draw state correlation diagrams, the possible reaction paths involved in eq 2 are investigated and listed in Table I. In this table, it is assumed that the reaction takes place via an intermediate similar to CP or CK, which is based on the suggestion by Willis and Bayes.[6] While the reaction path of eq 1 is obviously either linear or bent, that of eq 2 is very complicated. For easier understanding, the possible paths are given in Figure 1, and the most favorable path for each process is selected. The way of examining the reaction path by the state correlation diagrams is the same as that used previously.[8]

**Photodissociation of $C_3O_2$ in Equation 1.** Although the minimum-energy path of this reaction is already followed,[7] let us review it in terms of the correlation diagram. As Table I shows, there are two types of path in the photodissociation of $C_3O_2$. One is the least motion path which is the linear fragmentation of $C_{\infty h}$ symmetry. The other is the bent path of $C_s$ symmetry. While one of the dissociation products, $C_2O$, is expected to have several low-lying excited states, the other, CO, may be fixed to its ground state ($^1\Sigma^+$). The state correlation diagram for the linear fragmentation is given in Figure 2a. In this figure, the number displayed at both edges denotes the assignment of 34 electrons in a given configuration to each orbital ($\sigma$, $\pi_x$, and $\pi_y$). It is found that this path is symmetry disfavored in the ground state ($^1\Sigma_g^+$) and some low-lying excited states ($^3\Sigma_u^+$, $^{1,3}\Delta_u$, and $^{1,3}\Sigma_u^-$) owing to the avoided crossing. Figure 2b shows the correlation diagram for the bent path in which the $C_{\infty h}$ symmetry imposed on the reaction system is reduced to $C_s$ symmetry. As Figure 2b shows, the ground-state dissociation is still energetically unfavorable in the bent path. The dissociation in some excited states ($^3\Delta_u$ and $^{1,3}\Sigma_u^-$), however, becomes symmetry allowed in this pathway.

0002-7863/80/1502-0581$01.00/0 

**Table I.** List of Various Types of Reaction Paths Displayed in Figure 1

| reaction eq | no. | reaction scheme | type of reaction | pathways (symmetry of the system) |
|---|---|---|---|---|
| 1 | (1) | $C_3O_2 \rightarrow C_2O + CO$ | photodissociation of carbon suboxide | linear ($C_{\infty h}$)<br>bent ($C_s$) |
| | (2) | $C_2O + C_2H_4 \rightarrow C_4H_4O$ | addition of carbonyl-carbene to ethylene to form CK | I least motion ($C_{2v}$)<br>II bent-in-plane ($C_s$) ($X$-$Z$ symmetry plane)[a] |
| | (3) | $C_4H_4O \rightarrow C_3H_4 + CO$ | concerted (ring opening and elimination of CO) | III bent-out-of-plane ($C_s'$) ($Y$-$Z$ symmetry plane)[b] |
| 2 | (4) | $C_4H_4O \rightarrow C_3H_4 + CO$ | dissociation of CK to CP and CO | |
| | (5) | $C_3H_4 \rightarrow C_3H_4$ | ring opening of CP to form planar allene | IV conrotatory ($C_2$)<br>V disrotatory ($C_s$)<br>VI asymmetric ($C_1$) |
| | (6) | $C_3H_4 \rightarrow C_3H_4$ | intersystem crossing (CP → ground-state allene) without passing the excited-state allene | |
| | (7) | $C_3H_4 \rightarrow C_3H_4$ | intersystem crossing to form the ground-state allene | |

[a] See Figure 4. [b] See Figure 5.

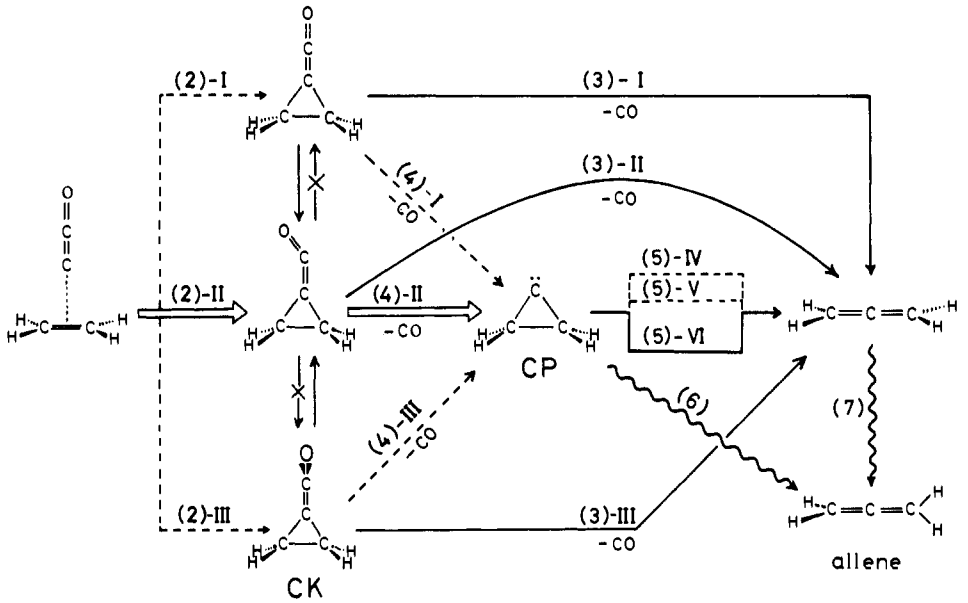


**Figure 1.** Possible mechanism for the reaction of eq 2. The routes in this figure are defined as the "reaction schemes" in Table I. In the right side of the figure, $T_1$ allene is assumed to have the planar and linear geometry, while its most stable structure is planar and bent. This assumption is needed so as to draw the state correlation diagram of the $C_{2v}$ symmetry in Figure 3a. Since the energy difference between linear and bent structures is small (~8 kcal/mol), the linear $T_1$ allene is used throughout the text.

It is found that the second excited state of $C_3O_2$ ($^3\Delta_u$) yields the ground-state $C_2O$ ($^3\Sigma^-$) and CO (the bold line in Figure 2b). The reaction path discussed here is in line with that of the previous calculation.[7] Thus, the "ground-state" $C_2O$ is generated through the bent path.

**Reaction of $C_2O$ with $C_2H_4$ in Equation 2. Schemes (2)-I → (3)-I and (2)-I → (4)-I.** Here, (2)-I denotes path (2) with $C_{2v}$ symmetry (see Table I). In the first process, the product allene is assumed to be of $C_{2v}$ symmetry.[9] Figure 3a shows the state correlation diagram for this process. Our attention is focused on the $^3A_2$ state, because the ground-state $C_2O$ ($^3\Sigma^-$) is involved in this state. It is found that in the $^3A_2$ state the scheme (2)-I is a symmetry-disfavored path because of the avoided crossing, while the scheme (3)-I of $^3$CK (i.e., triplet CK) → $^3C_3H_4$ + CO is a symmetry-allowed path. From this figure, the reaction path of the scheme (2)-I maintaining $C_{2v}$ symmetry is unfavorable and is ruled out. However, the schemes (3)-I, (3)-II, and (3)-III, the latter two of which have lower symmetry than $C_{2v}$, are found to be the symmetry-allowed paths. Figure 3b shows that the scheme (4)-I of the second process is symmetry disfavored.

**Schemes (2)-II → (4)-II.** In this process, the intermediacy of $^3$CK and $^3$CP is assumed. Figure 4 shows the state correlation diagram of $C_s$ symmetry for the process (2)-II → (4)-II, which is based on the correlation diagram of $C_{2v}$ symmetry exhibited in Figure 3. The curve connecting the lowest $^3$A states corresponds to the reaction of $C_2O(^3\Sigma^-) + C_2H_4 \rightarrow {}^3$CP + CO. As Figure 4 shows, schemes (2)-II → (4)-II give a symmetry-allowed path (bold line).

**Schemes (2)-III → (4)-III.** In this process, the intermediacy of $^3$CK and $^3$CP is again assumed. The correlation diagram of $C_s'$ symmetry for the schemes (2)-III and (4)-III is pictured in Figure 5. The curve connecting the $^3$A states corresponds to the reaction of $C_2O(^3\Sigma^-) + C_2H_4 \rightarrow {}^3$CP + CO. In this state, the scheme (2)-III is given a symmetry-disfavored path owing to the avoided crossing and the scheme (4)-III is unfa-

vorable because the $^3A$ state of CP is the high-lying state. Thus, the schemes (2)-III and (4)-III are ruled out from the possible reaction paths.

**Schemes (5)-IV, V, and VI.** In the ring opening of $^3CP$, the product $^3C_3H_4$ is assumed to have a bent planar structure ($C_{2v}$), which is the same as for Figure 3a. Figure 6a shows the correlation diagram of $C_2$ symmetry for the conrotatory ring opening. Our attention is focused on the curve connecting the $^3A$ state, which originates from the reaction of $C_2O(^3\Sigma^-) + C_2H_4$. As Figure 6a shows, the conrotatory ring opening is unfavorable because the $^3A$ state of the product $C_3H_4$ is the high-lying excited one. Figure 6b shows the correlation diagram of $C_s$ symmetry for the disrotatory ring opening. The $^3S$ state comes from the reaction of $C_2O(^3\Sigma^-) + C_2H_4$. As Figure 6b shows, the scheme (5)-V for the $^3S$ state is an energetically unfavorable path. From these results, the ring opening of $^3CP$ is considered to proceed along the asymmetric path [scheme (5)-VI]. However, the results of $^3CP \rightarrow {}^3C_3H_4$ calculated by Pasto et al. and Dillon and Underwood do not agree with this discussion.[10] In our analysis, the schemes (5)-IV and V are ruled out from the possible reaction paths.

Let us summarize the results obtained so far from the correlation diagrams. Some of the reaction schemes of eq 2 can be excluded either owing to the symmetry restriction or owing to the high-lying state energy and are indicated by the broken lines in Figure 1. Then the possible reaction schemes are reduced to the following five processes:

$$\text{(2)-II} \rightarrow \text{(4)-II} \rightarrow \text{(5)-VI} \rightarrow \text{(7)}$$

$$\text{(2)-II} \rightarrow \text{(4)-II} \rightarrow \text{(6)}$$

$$\text{(2)-II} \rightarrow \text{(3)-I} \rightarrow \text{(7)}$$

$$\text{(2)-II} \rightarrow \text{(3)-II} \rightarrow \text{(7)}$$

$$\text{(2)-II} \rightarrow \text{(3)-III} \rightarrow \text{(7)}$$

While the first step of eq 2 is expected to be the addition of $C_2O$ into $C_2H_4$ through the bent-in-plane path, further information on the probable path must be obtained from a quantitative analysis. Also, the intermediacy of CK and/or CP which is assumed in the qualitative discussion must be checked energetically. In the next section, the five possible reaction schemes are compared by ab initio calculations and the most probable process is sought.

## III. Results of the Minimum-Energy Path

The minimum-energy paths[11] for eq 2 are examined by the optimization procedure of the total energy ($E_T$). The $E_T$ of the reaction system of the triplet spin multiplicity is calculated by the GRHF method[12] with the STO-3G minimal basis set.[13]

**Scheme (2)-II.** This scheme is found to be symmetry favored in the previous section. The geometrical parameters to be optimized are shown in Figure 7a. As the result of calculations, the drawings of the optimized geometries and the potential-energy profile along the minimum-energy path are shown in Figures 8a and 8b, respectively.[14] Figure 8a shows that in the scheme (2)-II the $C_1 \cdots C_6$ bond is formed primarily and then the three-membered ring is formed. The energy profile shows a local minimum at $R \simeq 1.9$ Å which corresponds to a biradical intermediate. This intermediacy is found also in the photodissociation of cyclopropanone.[8b] It should be noted that in the energy profile of Figure 8b this reaction has no energy barrier.

**Schemes (3)-I,II and (4)-II.** These four schemes appear in the second step of eq 2 (the paths with full and bold lines in Figure 1). Since the most stable structure of $^3CK$ is the bent-in-plane type of $C_s$ symmetry, $^3CK$ of $C_{2v}$ symmetry and that of $C_s'$ symmetry have no minima. These geometries ($C_{2v}$ and $C_s'$) are merely models for comparison and such energetic instability makes the deformation ($C_s \rightarrow C_{2v}$ or $C_s'$) of CK improbable, which is indicated by two crosses attached to the vertical lines in Figure 1. Thus, the schemes (3)-I and (3)-III via the CK of $C_{2v}$ or $C_s'$ may be ruled out. Now the possible schemes of the decarbonylation are limited to the schemes (3)-II and (4)-II. In order to decide which scheme is more fa-

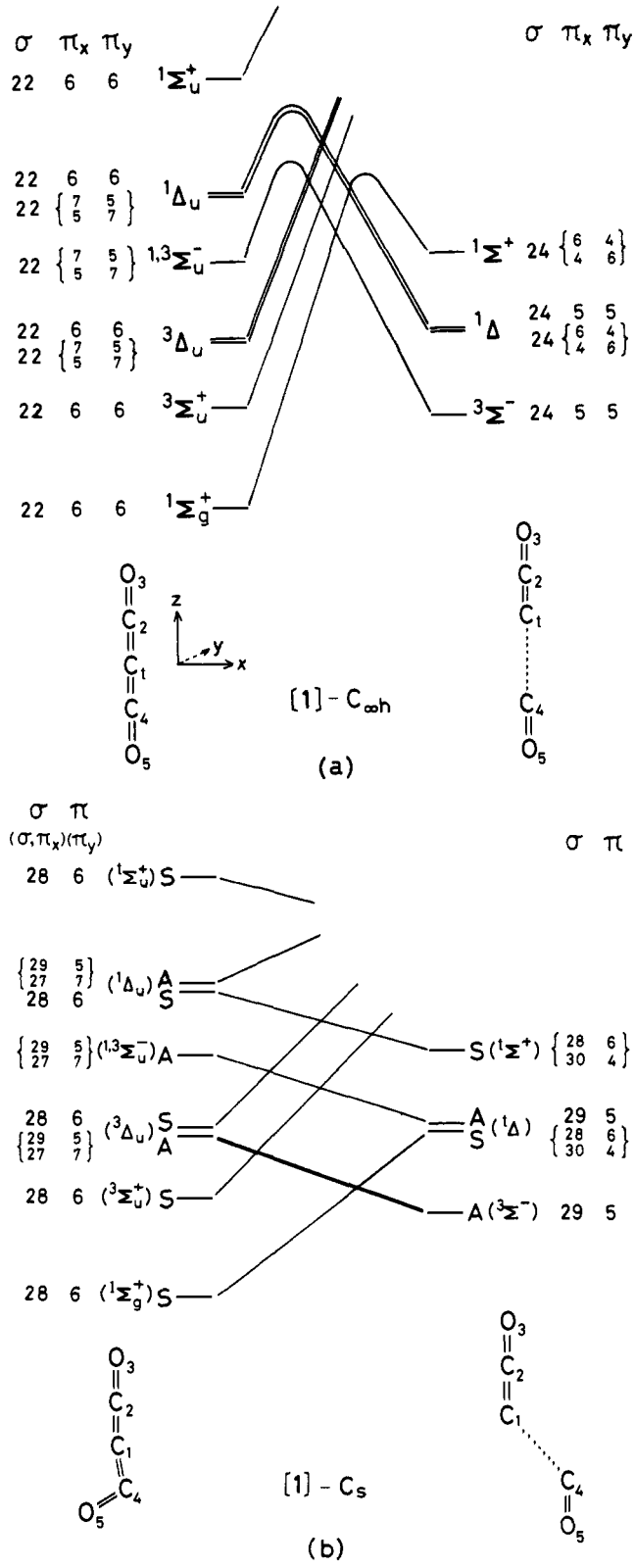


**Figure 2.** (a) The state correlation diagram for the linear fragmentation of $C_3O_2$ in eq 1. At both edges, the sets of numbers represent the number of electrons assigned to each MO. (b) The state correlation diagram for the bent dissociation of $C_3O_2$ in eq 1.

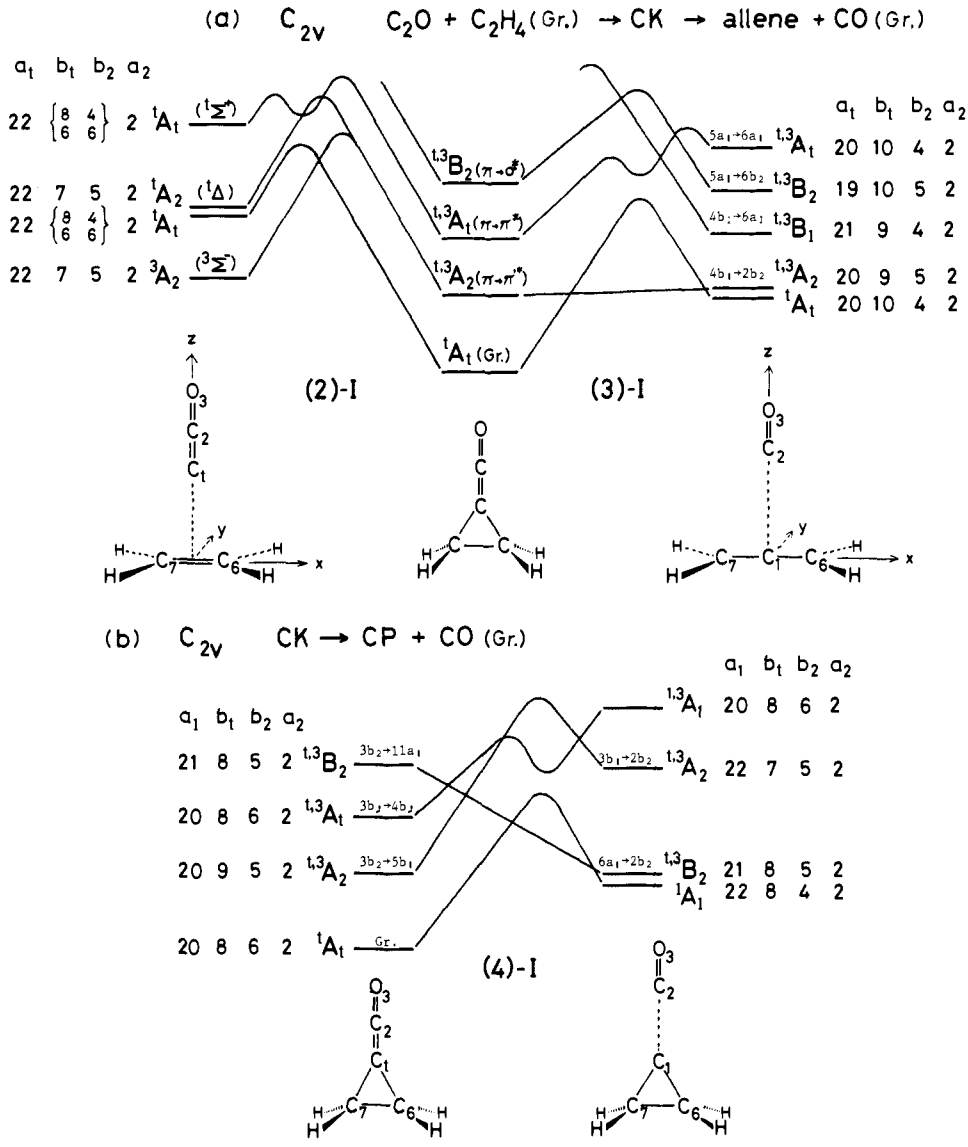


**Figure 3.** (a) The state correlation diagram of $C_{2v}$ symmetry for the schemes (2)-I → (3)-I in eq 2. (b) The state correlation diagram of $C_{2v}$ symmetry for the scheme (4)-I in eq 2. $C_2O(^3\Sigma^-)$ has the electron configuration . . . $(7a_1)^2(2b_1)^1(2b_2)^1(3b_1)^0(3b_2)^0(8a_1)^0$ . . . . The ground-state CK has the electron configuration . . . $(1a_2)^2(10a_1)^2(4b_1)^2(3b_2)^2(5b_1)^0(4b_2)^0(11a_1)^0$ . . . . The ground configuration of CP is . . . $(1a_2)^2(3b_1)^2(6a_1)^2(2b_2)^0(4b_1)^0$ . . . . The ground configuration of linear allene is . . . $(1a_2)^2(5a_1)^2(4b_1)^2(2b_2)^0(6a_1)^0(7a_1)^0$ . . . .

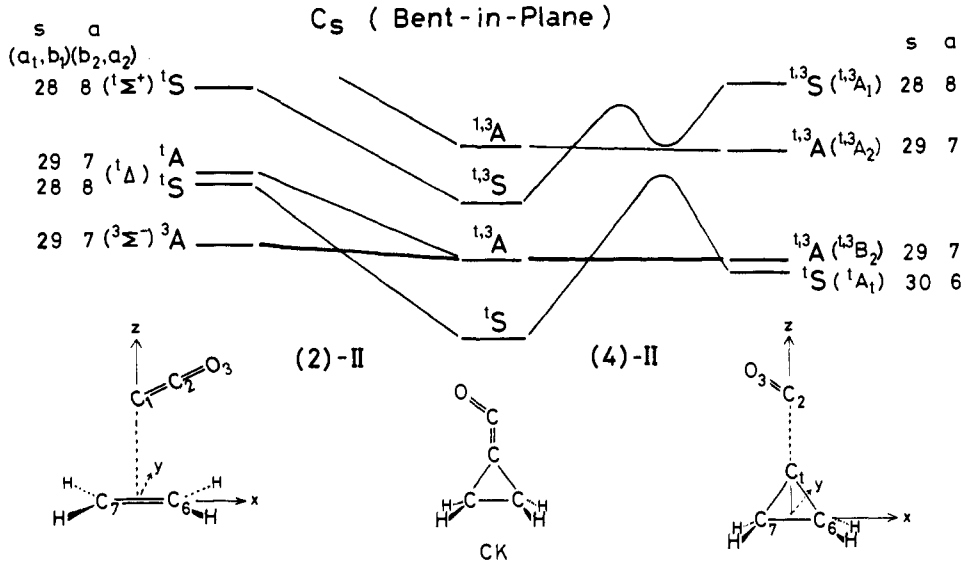


**Figure 4.** The state correlation diagram of $C_s$ symmetry for the schemes (2)-II → (4)-II in eq 2. The $C_{2v}$ symmetry imposed on the reacting system is reduced to $C_s$ symmetry.

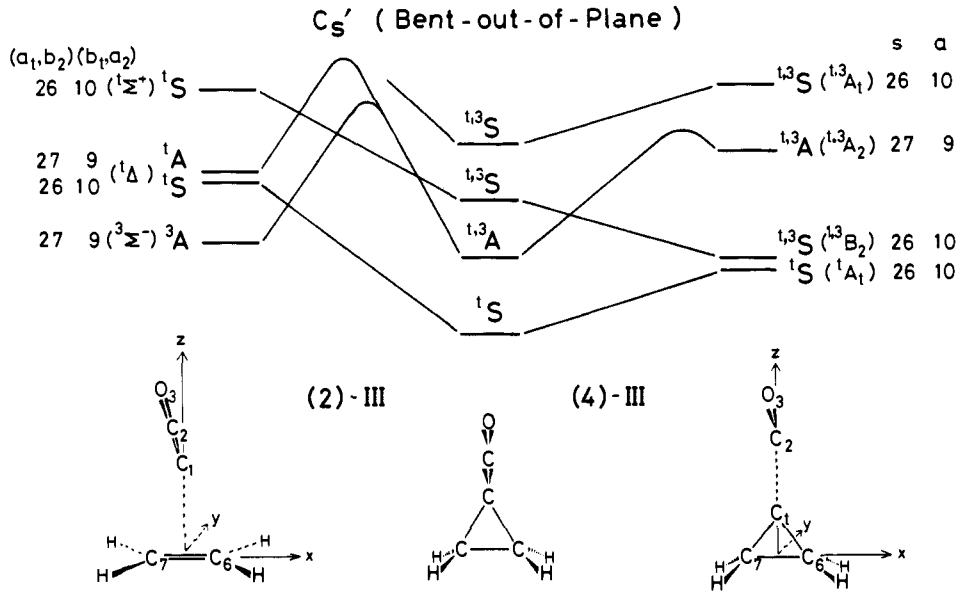


**Figure 5.** The state correlation diagram of $C_s'$ symmetry for the schemes (2)-III → (4)-III in eq 2. The $C_{2v}$ symmetry of the system is converted to $C_s'$ symmetry.

vorable, the minimum-energy path of the scheme (4)-II is first examined. The geometrical parameters are shown in Figure 7b. Here, the CP part of CK (i.e., three-membered ring) is kept frozen, because the geometry of the CP fragment is similar to that of the isolated CP according to our preliminary calculation. Figures 9a and 9b show drawings of the decarbonylation pathway and the potential-energy profile along the minimum-energy path. As Figure 9a shows, the decarbonylation ($^3$CK → $^3$CP + CO) takes the bent-in-plane path. This path is similar to that of the dissociation of the $(\pi,\pi^*)$ ketene.[8a]

Next, to see whether the path of the scheme (3)-II is energetically favorable or not, $E_T$ is calculated for the geometry with the elongated $C_1$-$C_2$ and $C_6$-$C_7$ bonds. The calculation for this "concerted" mechanism gives a much more unstable system than that of the scheme (4)-II (only the $C_1$-$C_2$ scission given). Thus, the possibility that the ($C_1$-$C_2$-$C_3$) ring opening and the dissociation of the $C_6$-$C_7$ bond take place simultaneously and cooperatively is more unlikely than that of the stepwise reaction. That is, the path of the scheme (4)-II is more favorable than that of the scheme (3)-II, which suggests that the reaction of eq 2 does pass the intermediate CP.

When the energetic superiority or inferiority is compared, two probable processes of eq 2 among the five symmetry-favored ones can be considered. One is the process (2)-II → (4)-II → (5)-IV → (7) and the other is the process (2)-II → (4)-II → (6). Since the $E_T$ of $^3$CP is lower than that of $^1$CP[9] and the $E_T$ of the planar $^3C_3H_4$ is appreciably high, the ground-state $C_3H_4$ may be yielded from $^3$CP by the intersystem crossing (isc). In this regard, the latter process is believed to be more likely than the former.

From the results of correlation diagrams and the calculation of $E_T$, the photochemical reaction of $C_3O_2$ with $C_2H_4$ is shown most likely to proceed through reacting steps (2)-II → (4)-II → (6). Here, the question of which step is rate determining should be answered. The energy barrier for the photodissociation of $C_3O_2$ in eq 1 is calculated to be about 18 kcal/mol,[7] and that of the decarbonylation of $^3$CK in Figure 9b is about 35 kcal/mol. Pasto et al. reported that the ring-opening step of $^3$CP has a 19 kcal/mol barrier with the 4-31G basis set and that of $^1$CP has 18 kcal/mol.[9] Comparing these energy values together with a small energy barrier of the scheme (2)-II, one may suggest that the rate-determining step of the overall reaction ($C_3O_2 + C_2H_4 \rightarrow C_3H_4 + 2CO$) is the decarbonylation of $^3$CK, i.e., the scheme (4)-II.

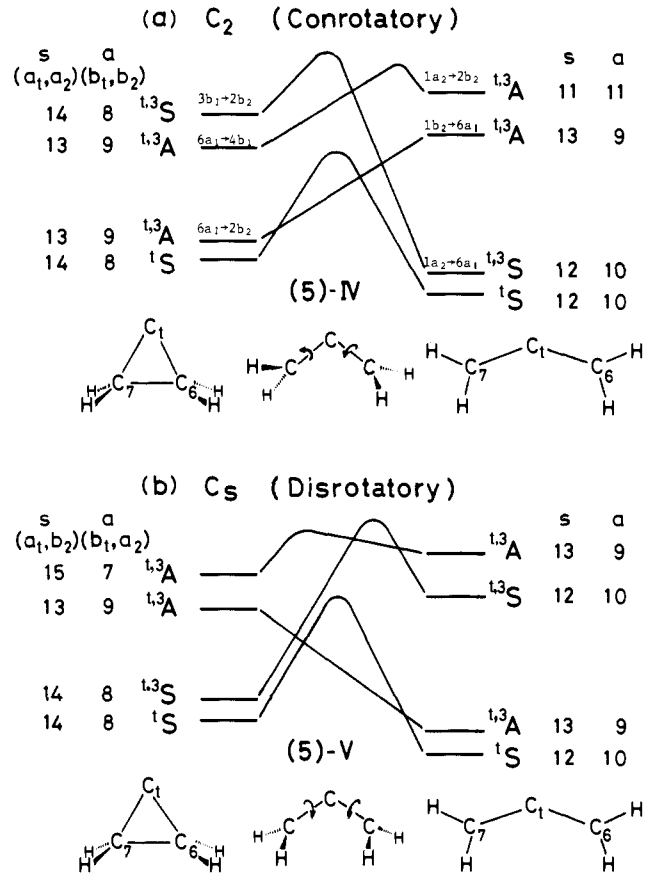


**Figure 6.** (a) The state correlation diagram of $C_2$ symmetry for the scheme (5)-IV in eq 2. (b) The state correlation diagram of $C_s$ symmetry for the scheme (5)-V in eq 2. The bent planar allene in the ground state has the electron configuration . . . $(4b_1)^2(1b_2)^2(1a_2)^2(6a_1)^0(2b_2)^0(7a_1)^0$ . . . .

## IV. Discussion Based on Orbital Interaction

The results of the correlation diagrams and the calculation of the $E_T$ suggest the favorable reaction schemes mentioned above. In this section, they are discussed in terms of the mode of orbital interaction.[15]

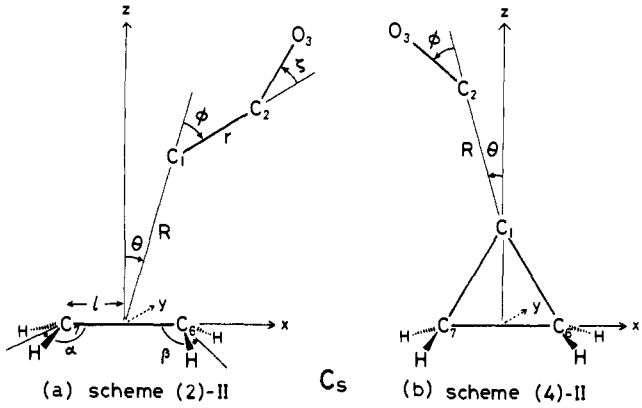


Figure 7. (a) Definition of the geometrical parameters to be optimized for obtaining the minimum-energy path for the scheme (2)-II. (b) The same for the scheme (4)-II.

**Photodissociation of $C_3O_2$ in Equation 1.** The motion of the leaving CO during the bent dissociation which is obtained by the energy optimization can be interpreted in terms of the orbital interaction scheme. The electron delocalization indicated by arrows in the following figure makes the reacting system stabilized. That is, the orientation of CO toward $C_2O$ given as

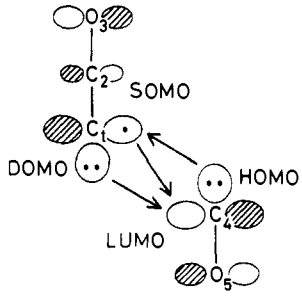


an energy-minimum point is in accord with that of the maximum overlapping interactions of the particular orbitals indicated in the following diagram. These particular orbitals are the doubly occupied (DO) MO, the highest occupied (HO) MO, the singly occupied (SO) MO, and the lowest unoccupied (LU) MO. Each orbital interaction between them is called a charge transfer (CT) interaction separately.

**Reaction of $C_2O$ with $C_2H_4$ in Equation 2.** In the previous section, the reaction of $C_2O$ with $C_2H_4$ is shown to involve the schemes (2)-II, (4)-II, and (6), where the former two schemes are traced by the ab initio calculations. The reaction mechanisms of the schemes (2)-II and (4)-II are now investigated.

**Scheme (2)-II.** In this reaction it is shown that the $C_1 \cdots C_6$ bond is formed primarily and then the three-membered ring is formed. This reaction process is explained by the CT and exchange ($E_K$) interactions. In the process of the $C_1 \cdots C_6$ bond formation, three types of CT ($CT_1$, $CT_2$, and $CT_3$) interactions given in the left side of the following figure contribute to the formation of the new bond. However, in the $C_1 \cdots C_7$ region, the

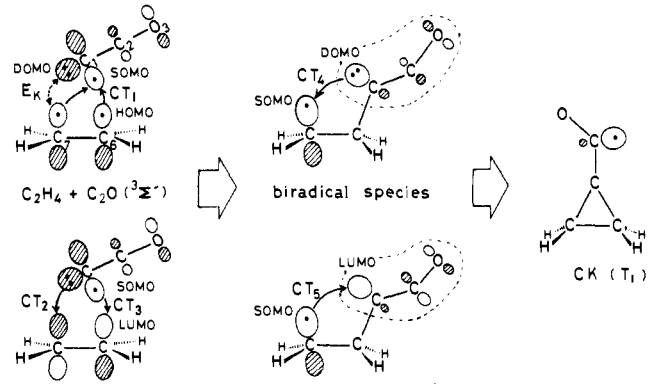


$E_K$ repulsion (dotted arrow) between the DOMO of $C_2O$ and the HOMO of $C_2H_4$ interferes with the $C_1 \cdots C_7$ bond formation, overcoming the attractive effect of $CT_2$. Consequently, the biradical species is formed. Next, $CT_4$ and $CT_5$ shown in the middle of the figure contribute to the formation of the three-membered ring.

The two unpaired electrons with parallel spins involved in the biradical intermediate in this process have an interesting behavior. While one of these unpaired electrons is localized almost at the $2p_y$ atomic orbital of the $C_1$ atom during the reaction of the scheme (2)-II, the other electron in the $X$-$Z$ plane moves from the $C_1$ atom of $C_2O$ to the $C_7$ atom of $C_2H_4$ and then from the $C_7$ atom to the $C_2$ atom of the former. This

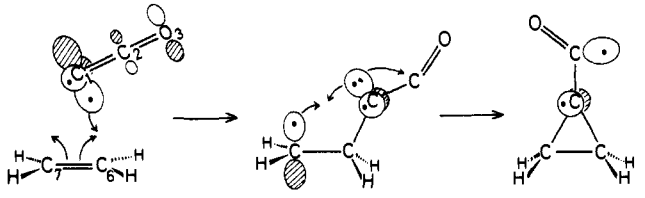

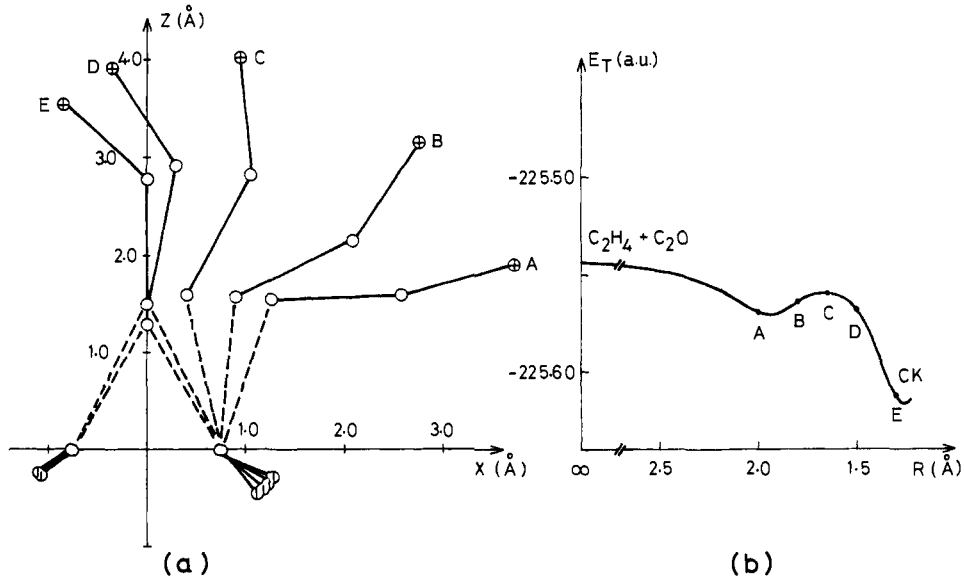


Figure 8. (a) The drawing of the optimized geometry for the scheme (2)-II. ○, ⊕, and ⊖ denote the carbon, oxygen, and hydrogen atoms, respectively (b) The potential-energy profile along the minimum-energy path for the scheme (2)-II.

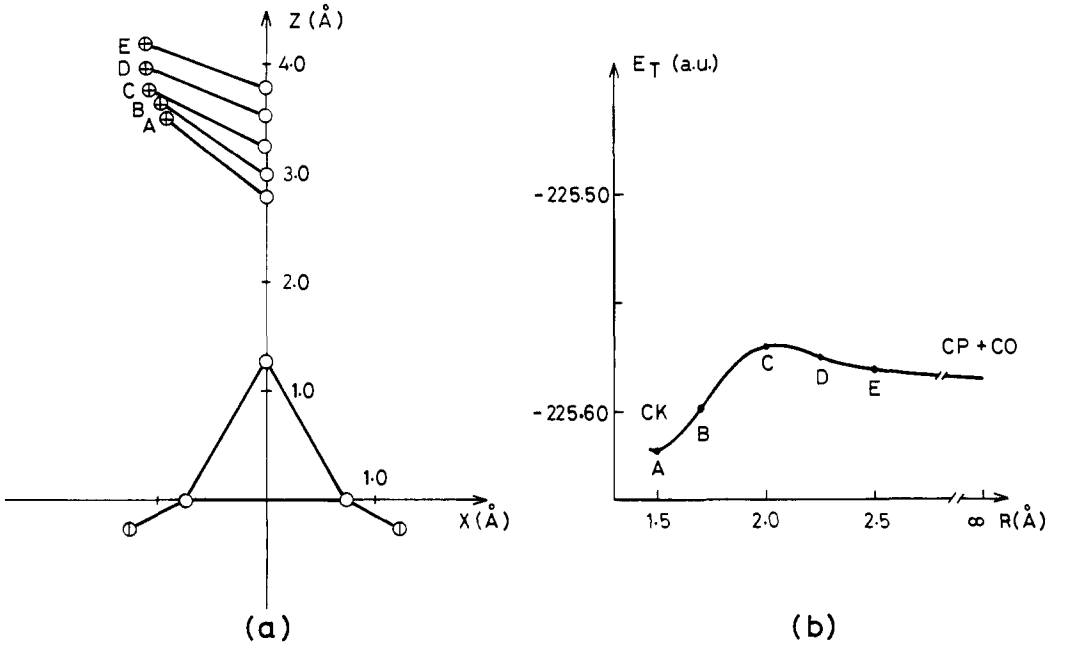


**Figure 9.** (a) The drawing of the optimized geometry for the scheme (4)-II. (b) The potential-energy profile along the minimum-energy path for the scheme (4)-II.

movement of the latter electron is explicable by the mode of orbital interaction.[16] The first movement ($C_1 \rightarrow C_7$) is brought about by the interaction of the SOMO of $C_2O$ with the $\pi$ and $\pi^*$ (HOMO and LUMO) orbitals of $C_2H_4$. The interaction of the SOMO with the $\pi$ and $\pi^*$ orbitals gives three orbitals ($\psi_1$, $\psi_2$, and $\psi_3$), where $\psi_2$ is the unpaired-electron orbital of

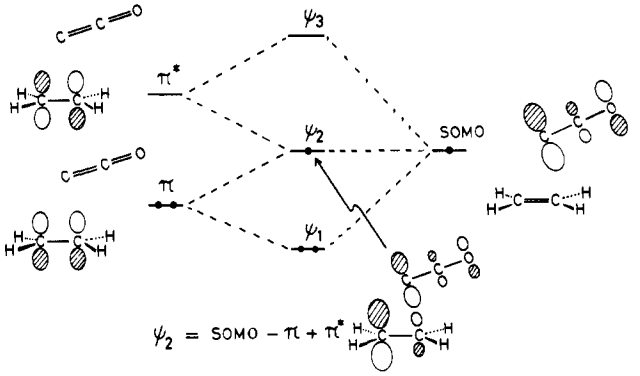


the reacting system. The $\psi_2$ orbital is represented as follows.[16]

$$\psi_2 = \text{SOMO} - \pi + \pi^*$$

The mixing of the $\pi$ and $\pi^*$ through the SOMO contributes to the spin transfer in the $C_1 \rightarrow C_7$ direction.

The movement ($C_7 \rightarrow C_2$) is also explicable by the interaction of the orbitals (SOMO of $C_7$, DOMO and LUMO of the $C_2O$ part in the biradical species) spreading over the region in which the new $C_1 \cdots C_7$ bond is formed. The interaction of the SOMO with the DOMO and the LUMO gives three orbitals ($\phi_1$, $\phi_2$, and $\phi_3$) where the $\phi_2$ orbital becomes the unpaired-electron orbital of the biradical intermediate. The $\phi_2$ orbital is also represented as follows:

$$\phi_2 = \text{SOMO} - \text{DOMO} + \text{LUMO}$$

Therefore, the mixing of the DOMO and the LUMO contributes to the ($C_7 \rightarrow C_2$) spin transfer.

**Scheme (4)-II.** Since the reaction of this scheme is shown to be the rate-determining step of the overall reaction, it is informative to clarify its reaction mechanism. The motion of the

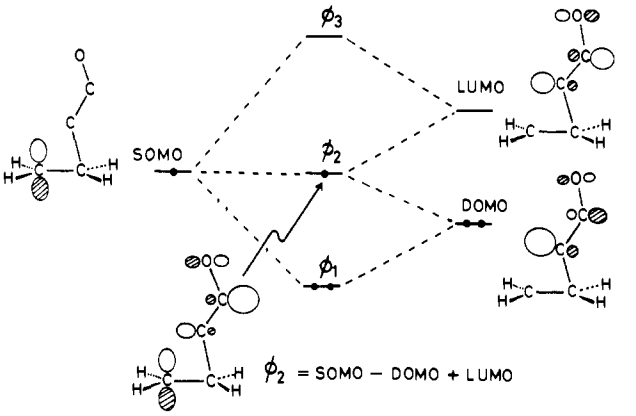


leaving CO in the decarbonylation obtained by the energy-optimized procedure is explained by the following CT interactions ($CT_6$, $CT_7$, $CT_8$, and $CT_8'$).

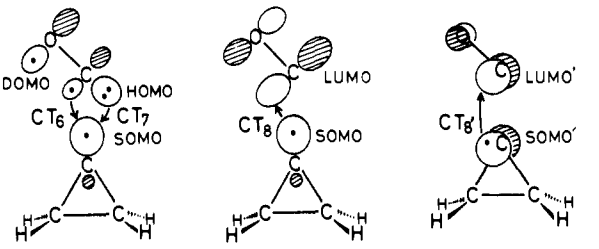


It should be noted that the LUMO of the CO fragment has a larger lobe at the C atom than at the O atom, whereas its DOMO has a larger lobe at the O atom. Therefore, $CT_8$ and $CT_8'$ are more important than $CT_6$. From the orientation of CO toward CP, it is considered that $CT_8$ is more important than $CT_7$. Consequently, CO is an electron acceptor. This result leads to a prediction that the scheme (4)-II proceeds more easily when the $C_2H_4$ fragment has an electron-donating substituent. This prediction is in line with the experimental result that the reactivity ($C_3O_2 + C_2H_4$) increases as the number of the methyl groups added to olefin increases.[5]

This reactivity in the scheme (4)-II is explained from another point of view.[15] The reaction may be initiated by the CT interaction between the ethylenic $\pi$-type bond ($C_6$–$C_7$) and

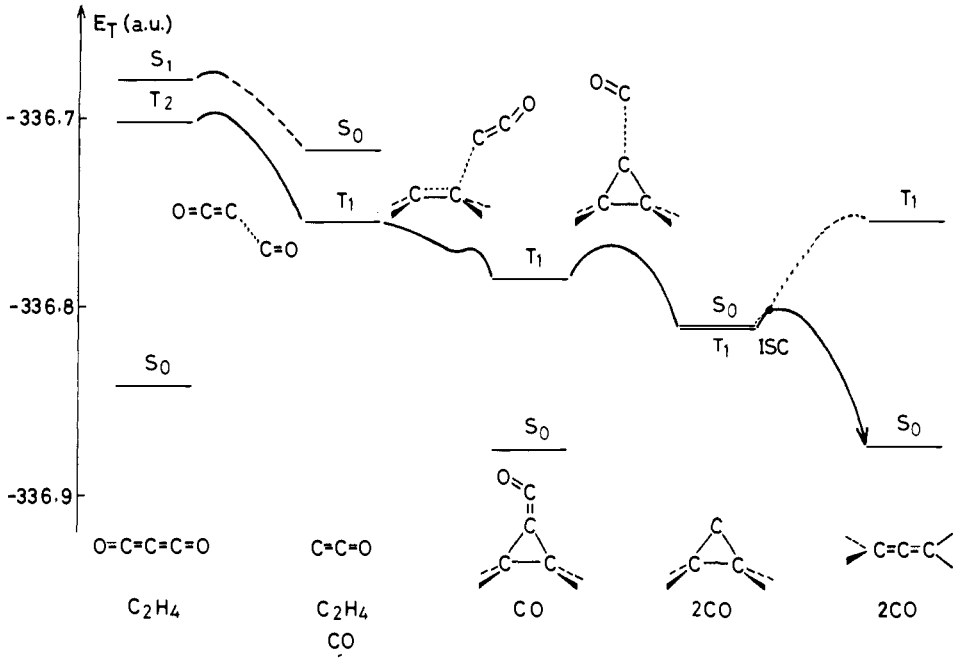


**Figure 10.** The summary of the photochemical reaction of $C_3O_2$ with $C_2H_4$ deduced from the present work. $E_T$ is calculated with the SECI method.

the $\sigma$ bond ($C_1$-$C_2$) to be broken. One of the SOMOs of the $C_2O$ part of the bent CK is localized at the $C_1$ and $C_2$ atoms and has the antibonding nature between them. The mode of the orbital interaction between the HOMO of the ethylenic part and the SOMO of the $C_2O$ part is depicted in the following figure.

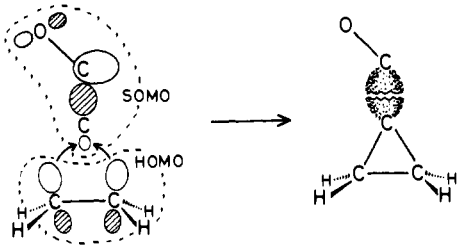


Since the back CT interaction from the SOMO to the LUMO of the ethylenic part does not contribute to the weakening of the $C_1$-$C_2$ bond due to the nodal property of the latter, the reaction may be initiated by the (HOMO → SOMO) CT interaction. This CT interaction is accelerated by the introduction of the electron-donating group to the $C_2H_4$ site, which explains the substituent effect on the overall reaction.

It should be noted that the scheme (2)-III apparently gives a favorable pathway according to the orbital interactions.

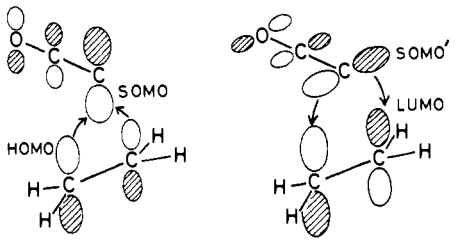


$C_s$' Bent - out - of - Plane

However, the state correlation diagram shown in Figure 5 indicates that the scheme (2)-III is a symmetry-disfavored path for the $^3A$ state owing to the avoided crossing. Therefore, even if a reaction path is favorable by the mode of the orbital interaction, it becomes unlikely in some excited states. When an excited state is studied, the states of the reacting and product sites should be correctly correlated. The method of the orbital interaction must be used after they are assigned. As is seen in this figure, in the bent-out-of-plane model the two odd electrons with the same spin are obligated to diffuse into the same region through the orbital interaction. This makes the model unfavorable. It is a well-established characteristic feature of the triplet-state reaction that two odd electrons tend to go away from each other to avoid the disadvantage due to the Pauli exclusion.[17]

## V. Concluding Remarks

In this work, the photochemical reaction of $C_3O_2$ with $C_2H_4$ is discussed by the use of the state correlation diagrams and ab initio calculations. Since $E_T$'s are calculated with a small basis set (STO-3G), energetics shown in Figures 8 and 9 are merely qualitative. However, some important results for this photochemical reaction are obtained and they are summarized schematically in Figure 10. In this figure, $E_T$ is recalculated by the singly excited configuration interaction (SECI) method to make uniform the energy scale of the overall reaction.

The multistep photochemical reaction of $C_3O_2$ with $C_2H_4$ seems to proceed as follows. The first step is evidently the photodissociation of $C_3O_2$ yielding $C_2O(^3\Sigma^-)$ and CO. This reaction takes the bent path. The next step is the addition of $C_2O$ to $C_2H_4$ through the bent-in-plane path, yielding $^3$CK.[18] It is decomposed into $^3$CP and CO through the bent-in-plane path. Since the $E_T$ of $^3$CP is lower than that of $^1$CP, the ground state $C_3H_4$ may be yielded from $^3$CP by the isc. The rate-determining step of the overall reaction is found to be the decarbonylation of $^3$CK. Thus, the intermediacy of $^3$CK and $^3$CP in the reaction of eq 2 is postulated.

**Acknowledgment.** The authors thank the Data Processing Center of Kyoto University for the allotment of the CPU time of the FACOM M-190 computer to them. They would like to express their gratitude to the Institute for Molecular Science for permission to use the HITAC M-180 computer.

## References and Notes

(1) (a) Kyoto University. (b) Osaka City University. (c) Nara University of Education.
(2) (a) Bayes, K. D. *J. Am. Chem. Soc.* **1962**, *84*, 4077. (b) Baker, R. T. K.; Kerr, J. A.; Trotman-Dickenson, A. F. *J. Chem. Soc. A* **1966**, 975.

(3) Mullen, R. T.; Wolf, A. P. *J. Am. Chem. Soc.* **1962**, *84*, 3214.
(4) Palmer, H. B.; Hirt, T. J. *J. Am. Chem. Soc.* **1962**, *84*, 113.
(5) Williamson, D. G.; Bayes, K. D. *J. Am. Chem. Soc.* **1968**, *90*, 1957.
(6) Willis, C.; Bayes, K. D. *J. Am. Chem. Soc.* **1966**, *88*, 3203.
(7) Osamura, Y.; Yamabe, S.; Minato, T.; Nishimoto, K. *Theor. Chim. Acta*, in press.
(8) (a) Yamabe, S.; Morokuma, K. *J. Am. Chem. Soc.* **1978**, *100*, 7551. (b) Yamabe, S.; Minato, T.; Osamura, Y. *Ibid.* **1979**, *101*, 4525.
(9) Pasto, D. J.; Haley, M.; Chipman, D. M. *J. Am. Chem. Soc.* **1978**, *100*, 5272.
(10) In ref 9, the ring-opening process is calculated by the UHF method and the following results are obtained. The ring opening occurs in three phases: (a) a nonrotatory process up to nearly the transition state with the $C_6$–$C_1$–$C_7$ bond angle $\simeq 90°$; (b) a rapid disrotatory motion around the transition state; (c) ring opening with gradual flattening of the methylenes to give the bent planar triplet allene. Although the path of the ring opening is shown in ref 9 to be disrotatory, Figure 6b shows that the disrotatory path is energetically disfavored. It should be noted that the UHF method gives the solution of the lowest triplet state and consequently the state of the initial stage of the reaction (S) becomes different from that of the final stage (A). Therefore, the ring opening may pass the asymmetric structure and then the state of the reacting system is switched (S → A). See also: Dillon, P. W.; Underwood, G. R. *J. Am. Chem. Soc.* **1977**, *99*, 2435.
(11) Each minimum-energy geometry is obtained with fixed distance between the $C_1$ of $C_3O_2$ and the center of the ethylenic $C_6$–$C_7$ bond or that between the $C_1$ and $C_2$ of $C_3O_2$ (Figure 7). "The minimum-energy path" in general does not agree with the "intrinsic reaction coordinate". See: Fukui, K; Kato, S.; Fujimoto, H. *J. Am. Chem. Soc.* **1975**, *97*, 1. Ishida, K.; Morokuma, K.; Komornicki, A. *J. Chem. Phys.* **1977**, *66*, 2153.
(12) (a) Davidson, E. R. *Chem. Phys. Lett.* **1973**, *21*, 565. (b) The GRHF program was coded by S. Iwata and K. Morokuma for the Rochester version of GAUSSIAN 70.
(13) The GAUSSIAN 70 program package is used for the $E_T$ calculation: Hehre, W. J.; Lathan, W. A.; Dichfield, R.; Newton, M. D.; Pople, J. A. Program No. 236, QCPE, Indiana University, Bloomington, Ind.
(14) In the initial state of the addition reaction, the GRHF (one configuration) wave function gives the unreasonable result of $E_T$ due to the configuration mixing. Then the calculation is restricted to the strongly interacting region. However, $C_2O$ is expected to attack $C_2H_4$ from the upper side, the $C_1$ of $C_2O$ being almost on the $Z$ axis.
(15) Fukui, K. *Acc. Chem. Res.* **1971**, *4*, 57.
(16) Inagaki, S.; Fujimoto, H.; Fukui, K. *J. Am. Chem. Soc.* **1976**, *98*, 4054.
(17) Kita, S.; Fukui, K. *Bull. Chem. Soc. Jpn.* **1969**, *42*, 66. Michl, J. *J. Am. Chem. Soc.* **1971**, *93*, 523. Zimmerman, H. E.; Epling, G. A. *Ibid.* **1972**, *94*, 3647. Fukui, K. "Theory of Orientation and Stereoselection"; Springer Verlag; West Berlin, 1975; p 81. Salem, L.; Bruckmann, P. *Nature (London)* **1975**, *258*, 526. Fukui, K.; Tanaka, K. *Bull. Chem. Soc. Jpn.* **1977**, *50*, 1391.
(18) When $^3CK$ is generated, it would be converted to $CK(S_0)$ through ISC. Even if $CK(S_0)$ appears in the course of the reaction, however, its dissociation is thought to be unlikely in consideration of the calculated result of ketene.[8a] In this sense, $CK(S_0)$, although in principle possible, would be excited again up to $CK(T_1)$ during the successive irradiation and the decomposition of $CK(S_0)$ to $CP(S_0)$ and CO would not take place.

# An Intermediate Neglect of Differential Overlap Technique for Spectroscopy of Transition-Metal Complexes. Ferrocene

**Michael C. Zerner,*[1a] Gilda H. Loew,[1b] Robert F. Kirchner,*[1b] and Ulrich T. Mueller-Westerhoff[1c]**

*Contribution from the Guelph-Waterloo Centre for Graduate Work in Chemistry, Department of Chemistry, University of Guelph, Guelph, Ontario N1G 2W1 Canada, the Department of Genetics, Stanford University Medical Center, Stanford, California 94305, and the IBM Research Laboratory, San Jose, California 95193.* *Received June 18, 1979*

**Abstract:** A new intermediate neglect of differential overlap (INDO-SCF-CI) method capable of calculating configuration interaction for transition-metal complexes is described. The technique is characterized by the use of atomic spectroscopic information in the formation of one-center, one-electron matrix elements and in the evaluation of two-electron integrals. All one-centered integrals that mix upon geometric rotations are found to be essential for calculation of configuration interaction and are retained. The method is applied to the calculation of the photoelectric and electronic spectra of ferrocene. Triplet and singlet state d → d* and charge-transfer transitions are considered. Three nearly degenerate triplet states are calculated for ferrocene at ~20 500 $cm^{-1}$ as compared to an observed triplet state at 18 900 $cm^{-1}$. Three singlet transitions of the d → d* type are calculated at 21 700, 23 900, and 31 900 $cm^{-1}$, in very good accord with the experimental observations and assignments of $^1E_1''$ at 21 800 $cm^{-1}$, $^1E_2''$ at 24 000 $cm^{-1}$, and $^1E_1''$ at 30 800 $cm^{-1}$. The lowest charge-transfer excitation is calculated at 36 900 $cm^{-1}$ compared to the experimental observation at 37 700 $cm^{-1}$. A considerable number of states above 36 900 $cm^{-1}$ are calculated and a possible assignment of the observed states in the higher energy region is given. The calculated energies allow spectral assignment in good agreement with experiment and help resolve prior ambiguities in the assignment. The relative energies calculated for the ionic states of the ferrocenium ion ($^3E_2' < {}^2A_1' < {}^2E_1''$) are in good accord with previous ab initio calculations. The first two of these states are formed from the formal loss of an electron from a metal orbital; the third, from the loss of an electron from a ligand orbital. For all of these states relaxation upon ionization is so significant that the net charge on iron increases only negligibly from +1.9 in ferrocene to +2.0 in the ferrocene ion. This observation is also in agreement with ab initio findings and has some support from Mössbauer spectroscopy.

## I. Introduction

To calculate the properties of organometallic transition-metal complexes from molecular orbital theory is often a difficult task. The number of integrals to be evaluated in an ab initio technique increases rapidly when a transition-metal atom is included in the molecule of interest. Care must be taken to treat in a consistent fashion the metal atoms and the organic moieties of the molecule. Extensive calculations often must be performed in order to explain differences between the normally localized metal orbitals and the typically delocalized ligand orbitals. It becomes of great interest therefore to develop a semiempirical model which can easily and successfully calculate properties of transition-metal complexes.

The electronic structure of transition-metal complexes has been described most frequently in terms of ligand field theory.[2a] Of great qualitative value, this approach is usually used

0002-7863/80/1502-0589$01.00/0 